SAR Data Statistical Description and Speckle Noise Filtering

Carlos López-Martínez, Eric Pottier

1 SAR Data Statistical Description

1.1 Introduction.

Most of geophysical media, as for instance: rough surfaces, vegetation, ice, snow, etc... have a very complicated structure and composition. Consequently, the knowledge of the exact scattered electromagnetic field, when illuminated by an incident wave, is only possible if a complete description of the scene was available. This type of description of the scatterers is unattainable for practical applications. The alternative, hence, is to describe them in a statistical form. Such scatters are named, consequently, as *distributed* or *partial scatters* [R16][R17], see previous chapter

SAR systems are mainly employed for natural scenes observation. Owing to the complexity of these targets, the scattered wave has also a complex behaviour. Hence, the scattering process itself needs too to be analyzed stochastically. Most of the techniques focused on solving the scattered wave problem try to find, hence, the statistical moments of the scattered field as a function of the incident wave properties, as well as, the scatterer features.

In order to derive a stochastic model for the observed SAR images in case of distributed scatterers, it is necessary to consider: a model for the SAR imaging process, a model for the scattering process and a model for the distributed scatter being imaged.

The SAR imaging process is divided into two main processes. The former consists of the acquisition of the scattered data, as a result of the illuminating wave, whereas the later comprises the focussing process. The second, which is in charge of collecting all the contributions of a particular scatterer focusing it as good as possible, tries to remove the effects of the acquisition process. The SAR impulse response, or SAR system model, embracing the acquisition, as well as, the focusing processes, can be assumed to be a rectangular low-pass filter [R18]

$$h(x,r) \propto \operatorname{sinc}\left(\frac{\pi x}{\delta_x}\right)\operatorname{sinc}\left(\frac{\pi r}{\delta_r}\right). \tag{1.1}$$

In the previous equation, x and r indicate the *azimuth* and *slant-range* (simply called range in the following) dimensions of the SAR image, respectively, whereas δ_x and δ_r indicate the spatial resolutions in the same spatial dimensions. Finally, a SAR image, i.e., $S(x,r)$, may be modelled as a two-dimensional low-pass filter, given by (1.1), applied to the scene's complex reflectivity $\sigma_s(x,r)$ [R18]

$$S(x,r) = \int_{-\infty}^{\infty}\int_{-\infty}^{\infty} \sigma_s(x',r')\,h(x-x',r-r')\,\mathrm{d}x'\mathrm{d}r'. \tag{1.2}$$

Since the spatial resolutions of the SAR impulse response, δ_x and δ_r are not zero, it is possible to introduce the concept of resolution cell as the area given by $\delta_x \times \delta_r$. Qualitatively, in the absence of signal re-sampling, the information contained by an image pixel, is basically determined by the average complex reflectivity $\sigma_s(x,r)$ within this resolution cell.

The resolution cell dimensions, δ_x and δ_r, are much larger than the wavelength of the illuminating electromagnetic wave λ. As a consequence, the resulting scattered wave is due to an elaborated scattering process. In order to arrive to a tractable mathematical model of the SAR image $S(x,r)$, it is convenient to find an approximation for the scattering process within the resolution cell. The most common simplification is the Born approximation or simple scattering approximation [R17][R19][R20][R21][R22]. Under it, first, the distributed scatterer is considered to be

composed by a set of discrete scatterers characterized by a deterministic response. This scatterer model might be reasonable for those cases in which the discrete scatterer description is valid, as for instance, scattering from raindrops or vegetation covered surfaces having leaves small compared with the wavelength. On the contrary, this assumption is not valid for continuous scatterers. In these cases, it is helpful to apply the concept of effective scattering centre [R16], in which the continuous scatterer is analysed in a discrete way, e.g., the facet model for surface scattering [R16][R23]. In a second step, the scattered wave from the resolution cell is supposed to be the linear coherent combination of the individual scattered waves of each one of the discrete scatters within the cell. The main limitation of the Born approximation is that it excludes attenuation or multiple scattering in the process.

Assuming the scattered wave from any distributed scatterer to be originated by a set of discrete sources, (1.2) can be considered in its discrete form

$$S(x,r)=\sum_{k=1}^{N}\sigma_s(x_k,r_k)\,h(x-x_k,r-r_k) \tag{1.3}$$

where the sub-index k refers to each particular discrete scatterer in the resolution cell, and N is the total number of these scatterers embraced by the response of the SAR system $h(x,r)$. Eq. (1.3) can be rewritten, by using

$$\sigma_s(x_k,r_k)=\sqrt{\sigma_k}\,\exp(j\theta'_{s_k}) \tag{1.4}$$

$$h(x-x_k,r-r_k)=h_k\exp(j\varphi_k) \tag{1.5}$$

$$\theta_{s_k}=\theta'_{s_k}+\varphi_k \tag{1.6}$$

where r denotes the amplitude and θ the phase, as follows

$$S(r,\theta)=\Re\{S\}+j\Im(S)=r\exp(j\theta) \tag{1.7}$$

where

$$r\exp(j\theta)=\sum_{k=1}^{N}A_k\exp(j\theta_{s_k}) \tag{1.8}$$

$$\Re\{S\}=\sum_{k=1}^{N}A_k\cos(j\theta_{s_k}) \tag{1.9}$$

$$\Im\{S\}=\sum_{k=1}^{N}A_k\sin(j\theta_{s_k}) \tag{1.10}$$

where $A_k=h_k\sqrt{\sigma_k}$. As observed in (1.8), the process to form a SAR image pixel consists of the complex coherent addition of the responses of each one of the discrete scatterers, which are not accessible individually. The sole available measure is the complex coherent addition itself. This coherent addition process receives the name of bi-dimensional *random walk* [R24][R25].

At this point, it is necessary to consider certain assumptions about the elementary scattered waves $A_k \exp\left(j\theta_{s_k} \right)$ in order to derive a stochastic model for the observed SAR image [R23][R26][R27]:

- The amplitude A_k and the phase θ_{s_k} of the kth scattered wave are statistically independent of each other and from the amplitudes and phases of all other elementary waves. This fact states that the discrete scatterers are uncorrelated and that the strength of a given scattered wave bears no relation to its phase.
- The phases of the elementary contributions θ_{s_k} are equally likely to lie anywhere in the primary interval $[-\pi, \pi)$.

Figure 1.1 – Radarsat-2 amplitude image of the scattering matrix element S_{hh} over San Francisco (USA).

Under these conditions, (1.8) may be seen as an interference process, in which the interference itself is determined by the phases θ_{s_k}. This interference can be constructive, as well as, destructive. This effect can be clearly noticed in SAR images, as the amplitude, or the intensity of (1.8) present a *salt and pepper* or *grainy* aspect, as it may be observed in Figure 1.1, which corresponds to $|S_{hh}|$ acquiered with the Radarsat-2 system over the city of San Francisco. Such a phenomenon is known as *speckle* [R28][R29][R30][R31].

Speckle is a true electromagnetic measurement and has a complete deterministic nature, as shown by (1.8). Nevertheless, the information contained within speckle needs from two different analyses. In those cases in which there is a reduced number of discrete scatterers within the resolution cell, or its response is basically originated by a reduced set of dominant ones, speckle is said to be *partially developed*. Hence, the interference itself, i.e., the speckle, contains information about the scattering process. On the contrary, when there are a large number of discrete scatterers in the cell, without a dominant one, the interference process becomes so complex, that it does contain almost no information about the scattering process itself [R32]. This case is called *fully developed speckle* [R17][R30], and the complexity of the interference process is overcome analyzing it by statistical means. Hence, speckle turns to be considered as a noise like signal [R28][R29][R30][R31].

Summarizing, due to the lack of knowledge about the detailed structure of the distributed scatterer being imaged by the SAR system, it is necessary to discuss the properties of the scattered field statistically. The statistics of concern are defined over an ensemble of objects, all with the same macroscopic properties, but differing in the internal structure. For a given SAR system imaging a particular scatterer, e.g., a rough surface, the exact value of each pixel cannot be

predicted, but only the parameters of the distribution describing the pixels values. Therefore, for a SAR image, the actual information per pixel is very low as individual pixels are random samples from distributions characterized by a reduced set of parameters.

1.2 One-dimensional Gaussian Distribution

Considering a SAR system to be described by a rectangular low-pass filter, see (1.1), and the distributed scatterer to be modelled by a set of discrete deterministic scatterers, by means of the single or Born scattering approximation, a SAR image, $S(x,r)$, can be described by the model presented by (1.8), (1.9) and (1.10).

The main parameter in the SAR image model is the number of discrete scatterers within the resolution cell, i.e., N. Depending on the nature of this parameter, different SAR image statistical models can be derived. On the one hand, if N is considered as a constant value, provided that it is large enough, (1.8), (1.9) and (1.10) lead to the complex, zero-mean, complex Gaussian pdf model, valid for homogeneous, non-textured SAR images [R23][R26][R27][R33]. On the other hand, to consider N as a random variable makes (1.8), (1.9) and (1.10) to lead to pdf models valid for textured areas description [R32]. In the following, the zero-mean, complex Gaussian distribution model shall be considered, despite possible extensions to textured image models shall be indicated.

When the number of discrete scatterers inside the resolution cell N is large, provided that $A_k \cos(j\theta_k)$ and $A_k \sin(j\theta_k)$ satisfy the *Central Limit Theorem* [R33], the quantities $\Re\{S\}$ and $\Im\{S\}$ are Gaussian distributed, that is, they follow a zero-mean, Gaussian pdf. The parameters of this pdf, can be obtained on the basis of the discrete scatterers model. The mean values of $\Re\{S\}$ and $\Im\{S\}$ are :

$$E\{\Re\{S\}\} = \sum_{k=1}^{N} E\{A_k \cos(\theta_k)\} = \sum_{k=1}^{N} E\{A_k\} E\{\cos(\theta_k)\} = 0 \tag{1.11}$$

$$E\{\Im\{S\}\} = \sum_{k=1}^{N} E\{A_k \sin(\theta_k)\} = \sum_{k=1}^{N} E\{A_k\} E\{\sin(\theta_k)\} = 0 \tag{1.12}$$

where $E\{x\}$ expresses the ensemble average. Using the same arguments, the variance values are obtained as

$$E\{\Re^2\{S\}\} = \sum_{k=1}^{N} E\{A_k^{\,2}\} E\{\cos^2(\theta_k)\} = \frac{N}{2} E\{A_k^{\,2}\} \tag{1.13}$$

$$E\{\Im^2\{S\}\} = \sum_{k=1}^{N} E\{A_k^{\,2}\} E\{\sin^2(\theta_k)\} = \frac{N}{2} E\{A_k^{\,2}\}. \tag{1.14}$$

Besides, the symmetry of the phase distribution of the discrete scatterers produces [R23]

$$E\{\Re\{S\}\Im\{S\}\} = \sum_{k=1}^{N}\sum_{l=1}^{N} E\{A_k A_l\} E\{\cos(\theta_k)\sin(\theta_l)\} = 0. \tag{1.15}$$

Under these conditions, $\Re\{S\}$ and $\Im\{S\}$, denoted in the following by *x* and *y*, respectively, are described by means of zero-mean Gaussian pdfs

$$p_x(x) = \frac{1}{\sqrt{\pi\sigma^2}} \exp\left(-\left(\frac{x}{\sigma}\right)^2\right) \quad x \in (-\infty, \infty) \tag{1.16}$$

$$p_y(y) = \frac{1}{\sqrt{\pi\sigma^2}} \exp\left(-\left(\frac{y}{\sigma}\right)^2\right) \quad y \in (-\infty, \infty) \tag{1.17}$$

where the variance is $\sigma^2 = (N/2)E\{A_k^2\}$. The pdfs $p_x(x)$ and $p_y(y)$ are denoted in the following as $\mathrm{N}(0, \sigma^2)$. Consequently, a SAR image, $S = x + jy = r\exp(j\theta)$, is described by a zero-mean, complex, Gaussian distribution, with uncorrelated real and imaginary parts, denoted next as $\mathrm{N}_{\mathbb{C}^2}(0, \sigma^2)$. From (1.16) and (1.17), it is straightforward to derive $p_r(r)$ and $p_\theta(\theta)$, where $r = \sqrt{x^2 + y^2}$ and $\theta = \arctan(y/x)$, as

$$p_{r,\theta}(r, \theta) = \frac{r}{\pi\sigma^2} \exp\left(-\left(\frac{r}{\sigma}\right)^2\right) \tag{1.18}$$

$$p_r(r) = \frac{2r}{\sigma^2} \exp\left(-\left(\frac{r}{\sigma}\right)^2\right) \quad r \in [0, \infty) \tag{1.19}$$

$$p_\theta(\theta) = \frac{1}{2\pi} \quad \theta \in [-\pi, \pi). \tag{1.20}$$

The amplitude pdf, i.e., $p_r(r)$, is known as *Rayleigh* distribution. In addition, if intensity, i.e., $I = r^2$, is considered, the Rayleigh pdf is transformed to an *exponential* pdf

$$p_I(I) = \frac{1}{\sigma^2} \exp\left(-\frac{I}{\sigma^2}\right) \quad I \in [0, \infty) \tag{1.21}$$

On the other hand, (1.20) shows that the SAR image phase has a uniform pdf. Consequently, this phase bears no information concerning the natural scene being imaged.

Given the SAR image amplitude pdf, (1.19), the amplitude mean value is equal to $\sigma\sqrt{\pi}/2$, whereas the variance equals $(1 - (\pi/4))\sigma^2$. If the coefficient of variation, defined as the standard deviation divided by the mean, is calculated, it equals $\sqrt{(4/\pi) - 1}$. For the intensity *I*, it has a value equal to 1 as the mean and the variance are equal to σ^2. As a consequence, the intensity of a SAR image can be modelled as the product of two uncorrelated [R26][R29][R30][R31], i.e.,

$$I = \sigma^0 n. \tag{1.22}$$

First, the deterministic-like value given by its mean, i.e., σ^0, which corresponds to the mean incoherent power of the area under study. Second, a random process n, with mean and variance equal to 1, characterized by an exponential

pdf. This second term is defined as the *speckle noise* component. As it may be observed from the model (1.21) and (1.22), if the mean value of the intensity increases, the variance increases as well. Therefore, this model is known as the *multiplicative* speckle noise model. In other words, the signal to noise ratio of the image cannot be improved by increasing the transmitted power as the variance of the data will increase proportionally.

The Gaussian model for SAR data, leading to (1.18) and (1.22), is able to characterize SAR data for homogeneous areas. In this case, useful information is described by a single degree of freedom, corresponding to the mean intensity. Nevertheless, for certain types of distributed scatterers, such a simple model cannot describe all the data variability. The reason behind this limitation is that this type of scatterers need from a more sophisticated model, with more than one degree of freedom, in order to be completely described. Collectively, these models are able to describe average intensity variations, which correspond to data texture [R32]. A variety of two-degree of freedom pdf models have been proposed in the literature, as for instance: K-distribution [R34], Weibull distribution or log-normal distribution [R35][R36][R37]. All these models consist of assuming the number of scatterers N, within a resolution cell, no longer as a constant, but being described also by a certain distribution. Even so, there are situations in which these two-parameter models are not able to describe the scene. Hence, the solution goes into the direction of introducing more degrees of freedom, thus, resulting into more elaborate image models [R32].

1.3 Multidimensional Gaussian Distribution

The previous section was concerned with the statistical description of one-dimensional complex data acquired by a complex SAR system, i.e., a single SAR image. As shown, despite the data's complex nature, only the amplitude, or the intensity, contain useful information concerning the distributed target under analysis. The amount of information can be increased by acquiring more than one SAR image, if one or more imaging parameters, e.g., system position, acquisition time, frequency or polarization, are varied. What it is pursued, hence, is the study of the variation of the scatterer's response to changes of the SAR system parameters. The volume of information is increased as more data channels are available, but also because, if available, the multidimensional data correlation structure can be also exploited to extract information about the observed scatterer [R32][R38]. The following list shows the most common multidimensional SAR configurations, as well as, the main application of them:

- *SAR Interferometry* (InSAR) [R50]: In this configuration, two SAR systems image the same scene from slightly different positions in space, leading to two-dimensional SAR data. In this way, the phase difference between the two acquisitions is proportional to the terrain's topography. This configuration is extensively employed nowadays to obtain Digital Elevation Models (DEMs) of the terrain.
- *Differential SAR Interferometry* (DinSAR) [R51]: This SAR configuration admits several variants. On the one hand, a differential interferogram can be obtained through the difference of two interferograms acquired with a zero spatial baseline, but at different times. Consequently, the "residual" differential interferogram can contain small topographic deformations or even atmospheric effects. On the other hand, the same effect can be observed if the topography of a given interferogram is compensated for by means of an external DEM.
- *SAR Polarimetry* (PolSAR) [R52]: In this case, the parameters which vary between the different information channels are: the polarization of the transmitted wave and the polarization with which the scattered wave by the terrain is collected. A set of two orthogonal polarization states are employed, being the most common the pair of horizontal and vertical polarizations. The most important property of polarimetry is that the polarimetric response to any polarization state of the incident wave of a given scatterer can be derived from the response to a pair of orthogonal polarization states. This SAR configuration exploits the fact that scatterers present different responses to different polarizations of the incident wave. For backscattering, in which waves are transmitted and collected in the same position and by considering the reciprocity theorem, PolSAR leads to three-dimensional data. On the contrary, when scattered waves are collected in a different position with respect to the transmitted one, i.e., forward scattering, PolSAR data are four-dimensional data.
- *Polarimetric SAR Interferometry* (PolInSAR) [R53]: This technique tries to combine both, the advantages of InSAR and PolSAR. On the one hand, the introduction of interferometric makes possible the data to be sensible to the structure of the target in the vertical dimension. On the other hand, the data are related to different scattering mechanisms in the same resolution cell thanks to the polarimetric capabilities of the acquisition system. Hence, PolInSAR data are sensible to different scattering mechanisms in the same image pixel, located at different heights. The introduction of simple scattering models allows to extract relevant information about the scatterer under study. Among the possible applications of this technique, the most

important is the extraction of parameters related with the vegetation cover which allow biomass estimation. In terms of data dimensionality, PolInSAR data consist of six-dimensional data if backscattering is considered, whereas they are eight-dimensional data for forward scattering.

- *SAR Tomography* (Multibaseline) [R54]: As shown in the previous point, PolInSAR represents a first step to resolve the vertical structure of the imaged scatterer. In this direction, SAR Tomography is a technique directed to achieve a real three-dimensional reconstruction of the scene being observation. Both, the SAR data acquisition and processing processes are based on the generation and processing of a synthetic aperture in the azimuth direction to reconstruct the object in this direction. In the same way, SAR tomography is based on the synthesis of an aperture in the dimension perpendicular to the plane formed by the azimuth and range dimensions, by acquiring several SAR images in the vertical dimension. Consequently, the phase information of these images can be employed to reconstruct, with enough spatial resolution, the vertical structure of the scatterer.
- Multifrequency SAR [R55][R56]: As shown in the literature, the response of a given scatterer depends on frequency. Consequently, in order to extract the maximum amount of information concerning the scatterer, several SAR images can be acquired at different frequencies. Therefore, the dimensionality of the data depends on the number of acquired images.

From a general point of view, a multidimensional SAR system acquires a set of SAR images, represented by the complex vector

$$\mathbf{k} = \left[S_1, S_2, \ldots, S_m\right]^T \tag{1.23}$$

where *m* represents the number of SAR images, i.e., the data dimensionality, according to the previous description. Each element of the vector $\mathbf{k}$, i.e., S_i for *i=1,2,...m*, represents a single complex SAR image. In PolSAR, the $\mathbf{k}$ receives the name of *scattering* or *target* vector (in the straightforward lexicographic basis), and it represents a vectorization of the scattering matrix $\mathbf{S}$ as detailed in previously. Considering that $S_i \sim \mathrm{N}_{\mathbb{C}^2}\left(0, \sigma^2\right)$, and assuming the *m* SAR images to be uncorrelated, i.e., independent, the pdf of $\mathbf{k}$ is

$$\begin{aligned} p_{\mathbf{k}}(\mathbf{k}) &= \prod_{k=1}^{m} \frac{1}{\pi\sigma^2} \exp\left(-\frac{S_k S_k^H}{\sigma^2}\right) = \frac{1}{\pi^m \sigma^{2m}} \exp\left(-\sum_{k=1}^{m} \frac{S_k S_k^H}{\sigma^2}\right) \\ &= \frac{1}{\pi^m \sigma^{2m}} \exp\left(-\frac{1}{\sigma^2} \mathrm{tr}\left(\mathbf{k}\mathbf{k}^H\right)\right). \end{aligned} \tag{1.24}$$

The correlation structure of the vector $\mathbf{k}$, provided that its *m* components $S_i \sim \mathrm{N}_{\mathbb{C}}\left(0, \sigma^2\right)$, is completely characterized by the Hermitian *covariance* matrix $\mathbf{C}$, defined as follows

$$\mathbf{C} = E\left\{\mathbf{k}\mathbf{k}^H\right\} = \begin{bmatrix} E\left\{S_1 S_1^H\right\} & E\left\{S_1 S_2^H\right\} & \cdots & E\left\{S_1 S_m^H\right\} \\ E\left\{S_2 S_1^H\right\} & E\left\{S_2 S_2^H\right\} & \cdots & E\left\{S_2 S_m^H\right\} \\ \vdots & \vdots & \ddots & \vdots \\ E\left\{S_m S_1^H\right\} & E\left\{S_m S_2^H\right\} & \cdots & E\left\{S_m S_m^H\right\} \end{bmatrix}. \tag{1.25}$$

Hence, in (1.24), the covariance matrix has been considered to be $\mathbf{C} = \sigma^2 \mathbf{I}_{m\times m}$, where $\mathbf{I}_{m\times m}$ represents the $m \times m$ identity matrix. Consequently, the model proposed in (1.24) is not able to take into consideration the correlation

structure of the multidimensional SAR data. In the particular case of PolSAR data, the data's correlation structure can be also expressed by the Hermitian *coherency* matrix $\mathbf{T}$ [R38].

As mentioned above, the main advantage of a multidimensional SAR system is the possibility to exploit the correlation structure characterizing a set of SAR images, in order to extract information about the scene being imaged. Consequently, the multidimensional SAR data model presented by (1.24) needs to be refined in order to describe a vector $\mathbf{k}$ characterized by a general correlation structure. Given an uncorrelated scattering vector $\mathbf{k}'$, whose pdf is given by (1.24), such that $E\left\{\mathbf{k}'\mathbf{k}'^{H}\right\}=\mathbf{I}_{m\times m}$, a correlated scattering vector $\mathbf{k}$can be defined as

$$\mathbf{k}=\mathbf{\Gamma}\mathbf{k}' \tag{1.26}$$

where the general covariance matrix is written as

$$\mathbf{C}=\mathbf{\Gamma}\mathbf{\Gamma}^{H}. \tag{1.27}$$

If the change of variable given by (1.26) is introduced within in (1.24), one can see that the complex vector $\mathbf{k}$ is characterized by the following pdf [R57][R58][R59]

$$p_{\mathbf{k}}(\mathbf{k})=\frac{1}{\pi^{m}|\mathbf{C}|}\exp\left(-\mathbf{k}^{H}\mathbf{C}^{-1}\mathbf{k}\right) \tag{1.28}$$

where $\mathbf{C}=E\left\{\mathbf{k}\mathbf{k}^{H}\right\}$. Hence, (1.28) represents the data pdf model for a set of *m* correlated SAR images, which is denoted in the following as $\mathrm{N}\left(\mathbf{0},\mathbf{C}\right)$. Since $\mathbf{k}\sim\mathrm{N}\left(\mathbf{0},\mathbf{C}\right)$, it is completely characterized by the first and the second central moments, i.e., the mean target vector and the covariance matrix, respectively.

At this point, it is important to consider, as presented by (1.11), (1.12) and (1.28), the issue that the mean value of the real and imaginary parts of $\mathbf{k}$equal zero. The main consequence is that it prevents the possibility to extract useful information via an estimation of this mean value. For instance, this circumstance determines the way PolSAR data has to be considered when distributed scatterers are of concern. A PolSAR system measures the 2×2 complex scattering matrix $\mathbf{S}$, which can be vectorized into the form presented by (1.23) [R38][R60], see also Section **Erreur ! Source du renvoi introuvable.**. On the one hand, when this scattering vector refers to a distributed scatterer, a given sample of it has almost no information concerning the scatterer itself, as $\mathbf{k}$ consists of a sample of the pdf given by (1.28) [R32]. On the other hand, if the mean value of $\mathbf{k}$ is estimated, it turns out to be zero. Thus, as reported in the literature, when distributed scatterers are studied, the vector$\mathbf{k}$, or the scattering matrix $\mathbf{S}$ in the particular case of PolSAR, cannot completely describe the properties of the distributed scatterer. Therefore, it is necessary to characterize these properties by means of higher order moments, i.e., through an estimation of the covariance matrix $\mathbf{C}$, or additionally, the coherency matrix $\mathbf{T}$. These two matrices are derived through the outer product of the target vectors $\mathbf{k}_l$ and $\mathbf{k}_p$, respectively, as indicated in Section **Erreur ! Source du renvoi introuvable.**, so they are independent of the absolute phase of the scattering matrix $\mathbf{S}$or the target vectors $\mathbf{k}_l$ and $\mathbf{k}_p$. Hence, the expected value in (1.25) needs to be estimated. The process to estimate the covariance matrix $\mathbf{C}$is also referred to as the polarimetric speckle noise process, as the objective is to remove the variability of the data making it possible to retrieve the $\mathbf{C}$ matrix.

In the rest, the complex, multidimensional Gaussian model, presented by (1.28), is taken as the multidimensional SAR imagery model. As for the one-dimensional model for a single SAR image, the complex, multidimensional Gaussian model can be considered valid for homogeneous areas, that is, areas in which the statistical properties of the data remain constant. The main reason of this choice has to be found in the fact that the simplicity of the complex, multidimensional Gaussian pdf, makes possible the analytical analysis of the information which can be extracted from the data. In addition, many studies reported in the literature support this model.

The multidimensional, zero-mean, complex Gaussian pdf model is based on the following assumptions:

- The distributed scatterer may be modelled as a collection of discrete, or point scatterers, whereas the scattering process occurring at the surface, or within it, is considered under the Born or simple scattering approximation.
- The properties of the distributed scatterer remain constant in space, hence, leading to homogeneous SAR data.

Thus, whenever any of the previous two suppositions are not fulfilled, SAR data cannot be longer assumed to be described by the complex, multidimensional Gaussian pdf model. These departures have been noticed in the literature at high resolutions or high frequencies, giving rise to data texture. As for one-dimensional SAR imagery, some of these departures can be explained by considering *N*, the total number of scatterers in the resolution cell, to be described by a certain pdf. If the mean number of scatterers contributing to the measurement at each pixel is large, then whatever the pdf of the number of discrete scatterers, the vector **k** can be represented by the product of two independent processes

$$\mathbf{k} = T\mathbf{k}' \tag{1.29}$$

Where T is a positive scalar texture and $\mathbf{k}'$ is a complex, multidimensional Gaussian distributed vector, with the same covariance as $\mathbf{k}$. When T is considered to be described by a square-root gamma pdf, the data $\mathbf{k}$ in (1.29) is described by the so called *K-distribution* [R34]. Despite (1.29) gives rise to textured data, an important result is that any model based on the fluctuation of the number of discrete scatterers within the resolution cell gives rise to data that is multivariate Gaussian at each pixel. That is, despite the texture, the data's correlation structure is still determined by the multidimensional Gaussian structure.

The main drawback of the model given by Eq. (1.29) is that, since the texture parameter *T* is an scalar, the texture information is the same of all the channels of the vector $\mathbf{k}$. Nevertheless, recent results presented in the literature, point out that, especially in the case of PolSAR data, the texture information could be different for every SAR data channel [R32][R61]. The physical reason that would explain this issue is that a scatterer presents different responses to different polarizations. Hence, these differences, of course considered in the covariance matrix $\mathbf{C}$, could be also be present within the texture information.

As noticed, in order to extract the useful information concerning the distributed scatterer under analysis from multidimensional SAR data, it is necessary to estimate the covariance matrix $\mathbf{C}$, or expressed in a different way, polarimeetric speckle noise must be filtered out. The estimated value of the covariance matrix $\mathbf{C}$, which generally receives the name of *sample covariance matrix* and is denoted by $\mathbf{Z}$, is studied in detail in the following. Previous to this analysis, it is necessary to reformulate (1.28) in order to consider multiple samples of the vector $\mathbf{k}$. By considering *n* samples of the vector $\mathbf{k}$, a new $mn\times 1$ vector $\mathbf{a}$ can be defined

$$\mathbf{a} = \left[\mathbf{k}_1^T, \mathbf{k}_2^T, \ldots, \mathbf{k}_n^T\right]^T \tag{1.30}$$

where every sample $\mathbf{k}_i$ has the structure given in (1.23). Since this new vector is an extension of the vector $\mathbf{k}$, it will be described by the zero-mean, multidimensional, complex Gaussian distribution, conveniently adapted to the new dimensionality of the vector. The main assumption that is made in this extension is that the *n* vectors $\mathbf{k}_i$, for *i=1,2,...m* are uncorrelated. Hence, the $mn \times mn$ complex covariance matrix of $\mathbf{a}$ can be written as

$$\mathbf{C}_\mathbf{a} = E\left\{\mathbf{a}\mathbf{a}^H\right\} = \begin{bmatrix} \mathbf{C} & \mathbf{0} & \cdots & \mathbf{0} \\ \mathbf{0} & \mathbf{C} & \cdots & \mathbf{0} \\ \vdots & \vdots & \ddots & \vdots \\ \mathbf{0} & \mathbf{0} & \cdots & \mathbf{C} \end{bmatrix} \tag{1.31}$$

where $\mathbf{C}$ is given by (1.25). As deduced from (1.31), the data in the vector $\mathbf{a}$ can be considered as homogeneous since the correlation properties of the samples $\mathbf{k}_i$ for *i=1,2,...m*, remain constant. Hence, the pdf of $\mathbf{a}$ is

$$p_{\mathbf{a}}(\mathbf{a}) = \frac{1}{\pi^{mn}|\mathbf{C}_{\mathbf{a}}|}\exp\left(-\mathbf{a}^H\mathbf{C}_{\mathbf{a}}^{-1}\mathbf{a}\right). \tag{1.32}$$

Eq. (1.32) can be simplified through a redefinition of both, the covariance matrix $\mathbf{C}_{\mathbf{a}}$, and $\mathbf{a}$. The $mn \times mn$ matrix $\mathbf{C}_{\mathbf{a}}$ can be written as

$$\mathbf{C}_{\mathbf{a}} = \mathbf{I}_{n\times n} \otimes \mathbf{C} \tag{1.33}$$

where $\otimes$ denotes the *matrix direct product* or *Kronecker product* of matrices. Hence,

$$|\mathbf{C}_{\mathbf{a}}| = |\mathbf{I}_{n\times n} \otimes \mathbf{C}| = |\mathbf{C}|^n. \tag{1.34}$$

On the other hand, $\mathbf{a}$ may be considered as the vectorization of a $m \times n$ matrix whose columns consist of the *n* vectors $\mathbf{k}_i$ for *i=1,2,...n* of $\mathbf{a}$, i.e.,

$$\begin{aligned}\mathbf{a} &= \left[\mathbf{k}_1^T, \mathbf{k}_2^T, \ldots, \mathbf{k}_n^T\right]^T = \mathrm{vec}\left(\left[\mathbf{k}_1, \mathbf{k}_2, \ldots, \mathbf{k}_n\right]\right) \\ &= \mathrm{vec}\left(\begin{bmatrix} S_{11} & S_{12} & \cdots & S_{1n} \\ S_{21} & S_{22} & \cdots & S_{2n} \\ \vdots & \vdots & \ddots & \vdots \\ S_{m1} & S_{m2} & \cdots & S_{mn} \end{bmatrix}\right) = \mathrm{vec}(\mathbf{A})\end{aligned} \tag{1.35}$$

where $\mathrm{vec}(\mathbf{X})$ indicates the operation of vectorization of the matrix $\mathbf{X}$. By introducing (1.34) and (1.35) in (1.32), the pdf of $\mathbf{a}$ is

$$p_{\mathbf{a}}(\mathbf{a}) = \frac{1}{\pi^{mn}|\mathbf{C}|^n}\exp\left(-\mathrm{vec}(\mathbf{A})^H\left(\mathbf{I}_{n\times n} \otimes \mathbf{C}\right)^{-1}\mathrm{vec}(\mathbf{A})\right). \tag{1.36}$$

The properties of the operators $\mathrm{vec}(\mathbf{A})$ and $\otimes$ allow to simplify the previous equation. Hence, the pdf of the vector $\mathbf{a}$, expressed as the matrix $\mathbf{A}$, takes the form

$$p_{\mathbf{A}}(\mathbf{A}) = \frac{1}{\pi^{mn}|\mathbf{C}|^n}\mathrm{etr}\left(-\mathbf{C}^{-1}\mathbf{A}\mathbf{A}^H\right). \tag{1.37}$$

where $\mathrm{etr}(\mathbf{X})$ is the exponential of the trace of the matrix $\mathbf{X}$. As performed with (1.28), the distribution of (1.37) is denoted by $\mathbf{A} \sim \mathrm{N}(\mathbf{0}, \mathbf{C})$.

1.4 The Wishart Distribution

The nature of multidimensional SAR data, provided the zero-mean, multidimensional, complex Gaussian pdf to be the right data model, makes necessary to study the distributed scatterer properties through the estimation of the covariance matrix $\mathbf{C}$. As given by (1.37), the distribution of the matrix $\mathbf{A}$, which corresponds to homogeneous, uncorrelated multidimensional SAR data samples, depends on the covariance matrix $\mathbf{C}$. Consequently, this pdf can be employed to derive the *Maximum Likelihood Estimation* (MLE) of $\mathbf{C}$[R32].

Given the pdf model of the data, in this case $p_{\mathbf{A}}(\mathbf{A})$, (1.37), the MLE for $\mathbf{C}$, denoted in the following by the matrix $\mathbf{Z}_n$, is the value of $\mathbf{C}$ maximizing $p_{\mathbf{A}}(\mathbf{A})$, where $\mathbf{A}$ is replaced by the observed data samples. Hence, the maximization process produces $\mathbf{Z}_n$ to be a function of $\mathbf{A}$, i.e., the covariance matrix is directly estimated from data. To consider $p_{\mathbf{A}}(\mathbf{A})$ as a function of $\mathbf{C}$, with $\mathbf{A}$ fixed, transforms it into the *likelihood function* [R62]. Often, it is easier to maximize the logarithm of $p_{\mathbf{A}}(\mathbf{A})$, called the *log-likelihood function* [R62], since the logarithm function is a monotone increasing function. The log-likelihood function of $p_{\mathbf{A}}(\mathbf{A})$ becomes

$$\ln\left(p_{\mathbf{A}}(\mathbf{A})\right) = -mn\ln(\pi) - n\ln\left(|\mathbf{C}|\right) + \mathrm{tr}\left(-\mathbf{C}^{-1}\mathbf{A}\mathbf{A}^{H}\right). \tag{1.38}$$

The maximum of (1.38) is found by making its derivative respect to $\mathbf{C}$ equal to zero. Acting in this way

$$\frac{\partial \ln\left(p_{\mathbf{A}}(\mathbf{A})\right)}{\partial \mathbf{C}} = -n\frac{\partial \ln\left(|\mathbf{C}|\right)}{\partial \mathbf{C}} + \frac{\partial\, \mathrm{tr}\left(-\mathbf{C}^{-1}\mathbf{A}\mathbf{A}^{H}\right)}{\partial \mathbf{C}} = 0. \tag{1.39}$$

In order to calculate the derivatives respect to $\mathbf{C}$, it must be considered that the covariance matrix is a complex matrix. Thus, the functions to be derived have to be complex differentiable, i.e., they have to satisfy the Cauchy-Riemman equations [R63]. Fortunately, both, the function $\ln\left(|\mathbf{C}|\right)$ and $\mathrm{tr}\left(-\mathbf{C}^{-1}\mathbf{A}\mathbf{A}^{H}\right)$ satisfy them. Using the following matrix derivatives rules

$$\frac{\partial |\mathbf{C}|}{\partial \mathbf{C}} = |\mathbf{C}|\left(\mathbf{C}^{-1}\right)^{H} \tag{1.40}$$

$$\frac{\partial\, \mathrm{tr}\left(-\mathbf{C}^{-1}\mathbf{A}\mathbf{A}^{H}\right)}{\partial \mathbf{C}} = -\left(\mathbf{C}^{-1}\right)^{H}\left(\mathbf{A}\mathbf{A}^{H}\right)^{H}\left(\mathbf{C}^{-1}\right)^{H} \tag{1.41}$$

one can conclude that the maximum of (1.38) is attained for

$$\mathbf{Z} = \frac{1}{n}\mathbf{A}\mathbf{A}^{H} \tag{1.42}$$

where the symbol $\mathbf{C}$ has been interchanged by $\mathbf{Z}$ in order to indicate that it corresponds to the MLE of the hermitian covariance matrix from data. By considering the definition of the matrix $\mathbf{A}$, (1.35), the MLE of the covariance matrix, (1.42), can be written as follows

$$\mathbf{Z}=\frac{1}{n}\mathbf{A}\mathbf{A}^{H}=\frac{1}{n}\begin{bmatrix} S_{11} & S_{12} & \cdots & S_{1n} \\ S_{21} & S_{22} & \cdots & S_{2n} \\ \vdots & \vdots & \ddots & \vdots \\ S_{m1} & S_{m2} & \cdots & S_{mn} \end{bmatrix}\begin{bmatrix} S_{11}^{*} & S_{21}^{*} & \cdots & S_{m1}^{*} \\ S_{12}^{*} & S_{22}^{*} & \cdots & S_{m2}^{*} \\ \vdots & \vdots & \ddots & \vdots \\ S_{1n}^{*} & S_{2n}^{*} & \cdots & S_{mn}^{*} \end{bmatrix}$$

$$=\begin{bmatrix} \frac{1}{n}\sum_{k=1}^{n}|S_{1k}|^{2} & \frac{1}{n}\sum_{k=1}^{n}S_{1k}S_{2k}^{*} & \cdots & \frac{1}{n}\sum_{k=1}^{n}S_{1k}S_{mk}^{*} \\ \frac{1}{n}\sum_{k=1}^{n}S_{2k}S_{1k}^{*} & \frac{1}{n}\sum_{k=1}^{n}|S_{2k}|^{2} & \cdots & \frac{1}{n}\sum_{k=1}^{n}S_{2k}S_{mk}^{*} \\ \vdots & \vdots & \ddots & \vdots \\ \frac{1}{n}\sum_{k=1}^{n}S_{mk}S_{1k}^{*} & \frac{1}{n}\sum_{k=1}^{n}S_{mk}S_{2k}^{*} & \cdots & \frac{1}{n}\sum_{k=1}^{n}|S_{mk}|^{2} \end{bmatrix}. \tag{1.43}$$

If one considers the expectation of the MLE

$$E\{\mathbf{Z}\}=\frac{1}{n}E\{\mathbf{A}\mathbf{A}^{H}\}=\mathbf{C} \tag{1.44}$$

it can be demonstrated that the MLE of the Hermitian covariance matrix is an unbiased estimator. In addition, it can be shown that the variance of the different matrix components of $\mathbf{Z}$ decrease with the number of samples n.

In SAR applications, the MLE of the covariance matrix receives often the name of covariance matrix *Multilook Estimator* [R62], whereas $\mathbf{Z}$ is known as the *Sample Covariance Matrix* [R32]. Here, *look* refers to each one of the independent averaged samples. Hence, it can be concluded from (1.44) that the performance of the covariance matrix estimation $\mathbf{Z}$, for homogeneous data, depends on the number of averaged samples or looks, in such a way, that the larger the number of looks, the lower the variance and the better the estimation. As the $\mathbf{Z}$ matrix is estimated from random samples, this matrix is also a random matrix. Finally, the distribution of the sample covariance matrix $\mathbf{Z}$ corresponds to the Wishart distribution

$$p_{\mathbf{Z}}(\mathbf{Z})=\frac{|\mathbf{Z}|^{n-m}}{|\mathbf{C}|^{n}\tilde{\Gamma}_{m}(n)}\operatorname{etr}\left(-\mathbf{C}^{-1}\mathbf{Z}\right) \tag{1.45}$$

where, the complex multivariate gamma function is defined as

$$\tilde{\Gamma}_{m}(n)=\pi^{m(m-1)/2}\prod_{i=1}^{m}\Gamma(n-i+1) \tag{1.46}$$

The distribution presented by (1.45) is denoted by $\mathbf{Z}\sim \mathrm{W}(n\mathbf{C},m)$. It can be observed from (1.45) that the Wishart distribution depends on three parameters: the number of data channels m, the number of averaged multidimensional data samples n and the true covariance matrix $\mathbf{C}$. The expression of the Wishart distribution is only defined for $n\geq m$ in order to assure $\mathbf{Z}$ to be a full-rank matrix with a non-zero determinant.

As it has been highlighted, the Hermitian covariance matrix $\mathbf{C}$ represents the cornerstone in multidimensional SAR data processing, and especially in PolSAR, together with its counterpart, the coherency matrix $\mathbf{T}$. The final objective of estimating these matrices is the possibility to extract physical information to characterize the distributed scatterers being imaged by the SAR system. This task is performed by a collection of algorithms and techniques, collectively known as *Inversion Algorithms*. The aim of these techniques is the establishment of relations between the physical properties of the distributed scatterer and the observed SAR data, hence, making it possible the inversion of this

process in order to extract physical information from observed multidimensional SAR data. Most of these techniques have the covariance matrix $\mathbf{C}$, or certain information derived from it, as the main input of the inversion process. Since due to the intrinsic nature of SAR systems, direct access to the covariance matrix $\mathbf{C}$ is not possible, it must be estimated from the observed multidimensional SAR data.

As shown in Section 1.2, the estimation of incoherent power may be also understood as a filtering process. One alternative to define this filtering process is to assume a given noise model able to identify the information of interest and the noise sources that corrupt this information. In case of single SAR images, this noise model corresponds to the multiplicative speckle noise model in (1.22). In the case of multidimensional SAR data, this model cannot be extended the whole covariance matrix $\mathbf{Z}$ as it would imply uncorrelated SAR images, as expressed in (1.24). Nevertheless, the multiplicative speckle noise model can be extended to model the diagonal, as well, as the off-diagonal elements of $\mathbf{Z}$ [R71][R72]. In this case, the nature of the speckle noise for a particular element of the covariance matrix depends on the correlation that characterizes this element. For low correlation, speckle noise presents an additive nature, whereas for high correlation, speckle noise is characterized by a multiplicative behaviour. Consequently, this model is referred to as the *multiplicative-additive* speckle noise model for multidimensional SAR data.

As shown in Section 1.2, the estimation of incoherent power may be also understood as a filtering process. One alternative to define this filtering process is to assume a given noise model able to identify the information of interest and the noise sources that corrupt this information. In case of single SAR images, this noise model corresponds to the multiplicative speckle noise model in (1.22). In the case of multidimensional SAR data, this model cannot be extended the the whole covariance matrix $\mathbf{Z}$ as it would imply uncorrelated SAR images, as expressed in (1.24). Nevertheless, the multiplicative speckle noise model can be extended to model the diagonal, as well, as the off-diagonal elements of $\mathbf{Z}$ [R71][R72]. In this case, the nature of the speckle noise for a particular element of the covariance matrix depends on the correlation that characterizes this element. For low correlation, speckle noise presents an additive nature, whereas for high correlation, speckle noise is characterized by a multiplicative behaviour. Consequently, this model is referred to as the *multiplicative-additive* speckle noise model for multidimensional SAR data.

1.5 The Polarimetric Covariance and Coherence Matrices

As indicated in the previous section, the characterization of distributed scatterers must be performed through the covariance $\mathbf{C}$ or the coherency $\mathbf{T}$ matrices. In a bistatic configuration, and according to what has been presented in Section **Erreur ! Source du renvoi introuvable.**, these two matrices are defined as

$$\mathbf{C} = E\left\{\mathbf{k}_l \mathbf{k}_l^{T*}\right\} = \begin{bmatrix} E\left\{|S_{hh}|^2\right\} & E\left\{S_{hh}S_{hv}^*\right\} & E\left\{S_{hh}S_{vh}^*\right\} & E\left\{S_{hh}S_{vv}^*\right\} \\ E\left\{S_{hv}S_{hh}^*\right\} & E\left\{|S_{hv}|^2\right\} & E\left\{S_{hv}S_{vh}^*\right\} & E\left\{S_{hv}S_{vv}^*\right\} \\ E\left\{S_{vh}S_{hh}^*\right\} & E\left\{S_{vh}S_{hv}^*\right\} & E\left\{|S_{vh}|^2\right\} & E\left\{S_{vh}S_{vv}^*\right\} \\ E\left\{S_{vv}S_{hh}^*\right\} & E\left\{S_{vv}S_{hv}^*\right\} & E\left\{S_{vv}S_{vh}^*\right\} & E\left\{|S_{vv}|^2\right\} \end{bmatrix} \tag{1.47}$$

and

$$\mathbf{T} = \mathbf{k}_p \mathbf{k}_p^{T*} = \begin{bmatrix} E\left\{|S_{hh}+S_{vv}|^2\right\} & E\left\{(S_{hh}+S_{vv})(S_{hh}-S_{vv})^*\right\} & E\left\{(S_{hh}+S_{vv})(S_{hv}+S_{vh})^*\right\} & E\left\{(S_{hh}+S_{vv})(j(S_{hv}-S_{vh}))^*\right\} \\ E\left\{(S_{hh}-S_{vv})(S_{hh}+S_{vv})^*\right\} & E\left\{|S_{hh}-S_{vv}|^2\right\} & E\left\{(S_{hh}-S_{vv})(S_{hv}+S_{vh})^*\right\} & E\left\{(S_{hh}-S_{vv})(j(S_{hv}-S_{vh}))^*\right\} \\ E\left\{(S_{hv}+S_{vh})(S_{hh}+S_{vv})^*\right\} & E\left\{(S_{hv}+S_{vh})(S_{hh}-S_{vv})^*\right\} & E\left\{|S_{hv}+S_{vh}|^2\right\} & E\left\{(S_{hv}+S_{vh})(j(S_{hv}-S_{vh}))^*\right\} \\ E\left\{j(S_{hv}-S_{vh})(S_{hh}+S_{vv})^*\right\} & E\left\{j(S_{hv}-S_{vh})(S_{hh}-S_{vv})^*\right\} & E\left\{j(S_{hv}-S_{vh})(S_{hv}+S_{vh})^*\right\} & E\left\{|S_{hv}-S_{vh}|^2\right\} \end{bmatrix} \tag{1.48}$$

respectively. In the case of a monostatic system configuration, the covariance and the coherency matrices are defined as

$$\mathbf{C} = E\left\{\mathbf{k}_l \mathbf{k}_l^{T*}\right\} = \begin{bmatrix} E\left\{|S_{hh}|^2\right\} & E\left\{\sqrt{2}S_{hh}S_{hv}^*\right\} & E\left\{S_{hh}S_{vv}^*\right\} \\ E\left\{\sqrt{2}S_{hv}S_{hh}^*\right\} & E\left\{|S_{hv}|^2\right\} & E\left\{\sqrt{2}S_{hv}S_{vv}^*\right\} \\ E\left\{S_{vv}S_{hh}^*\right\} & E\left\{\sqrt{2}S_{vv}S_{hv}^*\right\} & E\left\{|S_{vv}|^2\right\} \end{bmatrix} \tag{1.49}$$

and

$$\mathbf{T} = E\left\{\mathbf{k}_p \mathbf{k}_p^{T*}\right\} = \begin{bmatrix} E\left\{|S_{hh}+S_{vv}|^2\right\} & E\left\{(S_{hh}+S_{vv})(S_{hh}-S_{vv})^*\right\} & E\left\{2(S_{hh}+S_{vv})S_{hv}^*\right\} \\ E\left\{(S_{hh}-S_{vv})(S_{hh}+S_{vv})^*\right\} & E\left\{|S_{hh}-S_{vv}|^2\right\} & E\left\{2(S_{hh}-S_{vv})S_{hv}^*\right\} \\ E\left\{2S_{hv}(S_{hh}+S_{vv})^*\right\} & E\left\{2S_{hv}(S_{hh}-S_{vv})^*\right\} & E\left\{4|S_{hv}|^2\right\} \end{bmatrix} \tag{1.50}$$

In the previous four definitions, the term $E\{\cdot\}$ refers to the expectation operator that needs to be estimated from the data samples. As demonstrated in the previous section, the maximum likelihood estimator of this operator, and therefore the maximum likelihood estimator of the covariance and coherency matrices correspond to the spatial averaging, referred to as *Multilook* or *Boxcar* filter. In this case, the estimated covariance and coherency matrices receive the names of sample covariance and sample coherency matrices, respectively.

Eqs. (1.49) and (1.50) represent the most general form of the covariance and coherency matrices, respectively, for a monostatic configuration. As these matrices are Hermitian, they contain up to nine independent parameters. Nevertheless, depending on the type of scatterer, the number of independent parameters can be lower leading to a particular for of the covariance $\mathbf{C}$ or the coherency $\mathbf{T}$ matrices. It the the scatterer under study has reflection symmetry in a plane normal to the line of sight then the covariance and the coherency matrices will have the following general forms

$$\mathbf{C} = \begin{bmatrix} x & 0 & x \\ 0 & x & 0 \\ x & 0 & x \end{bmatrix} \qquad \mathbf{T} = \begin{bmatrix} x & x & 0 \\ x & x & 0 \\ 0 & 0 & x \end{bmatrix} \tag{1.51}$$

that is, the crosspolar scattering coefficient will be uncorrelated with the copolar terms. Under this hypothesis, the covariance $\mathbf{C}$ or the coherency $\mathbf{T}$ matrices present up to five independent parameters. In addition to reflection symmetry, a medium may also exhibit rotation symmetry. This type of symmetry is referred to as azimuthal symmetry, leading to a coherency matrix presenting the following form

$$\mathbf{T} = 2\begin{bmatrix} \alpha & 0 & 0 \\ 0 & \beta & 0 \\ 0 & 0 & \beta \end{bmatrix} \tag{1.52}$$

Which has only two independent parameters α and β.

1.6 The Polarimetric Coherence

From the expressions of the covariance and coherency matrices that were introduced previously, one may see that the elements of these matrices may be divided into two types. On the one hand, the diagonal elements containing the power information, and on the other hand the off-diagonal elements that contain the correlation information between the different channels of information. This correlation information may be considered in an absolute way by considering just the off-diagonal elements of these matrices. Nevertheless, this correlation information may be also considered in a relative way through the so-called complex correlation parameter, defined as

$$\rho = \left|\rho e^{j\phi_x}\right| = \frac{E\left\{S_k S_l^*\right\}}{\sqrt{E\left\{\left|S_k\right|^2\right\} E\left\{\left|S_l\right|^2\right\}}} \tag{1.53}$$

This parameter contains the information of statistical resemblance between any two SAR images S_k and S_l. Indeed, these SAR images correspond to the different elements of the target vector $\mathbf{k}$ defined in Section **Erreur ! Source du renvoi introuvable.**. The amplitude of the complex correlation coefficient, normally referred to as correlation $|\rho|$ presents a value in the range [0, 1]. If $|\rho| = 0$ means that both SAR images are statistically independent and the phase information ϕ_x contains no information. For $|\rho| = 1$, both SAR images are statistically equal and the phase information, free of noise, is a delta function containing information about the scattering process. For any other value, $|\rho|$ establishes the correlation between both SAR images and the phase information ϕ_x is contaminated by the effect of speckle noise.

In multidimensional SAR imagery, the complex correlation coefficient has been revealed as an important source of information. In particular, the correlation coefficient amplitude, named coherence, apart to depend on the SAR system characteristics, it is also influenced by the physical properties of the area under study. The complex correlation coefficient is the most important observable for SAR interferometry (InSAR) [R50]. On the one hand, and considering the acquisition geometry, it has been demonstrated that its phase contains information about the Earth's surface topography. Therefore, InSAR phase data are employed to derive Digital Elevation Models (DEMs) of the terrain. On the other hand, despite there is not a complete understanding about the parameters and the physical processes affecting the interferometric coherence, it has been shown that this parameter may be successfully employed to characterize the properties and the dynamics of the Earth's surface.

The coherence represents also an important source of information when PolSAR data are addressed. In particular, the complex correlation coefficient parameter derived from circularly polarized data has been employed to characterize rough surfaces [R64], to study the sea surface [R65] or to discriminate sea ice types [R66]. When obtained from linearly polarized data, the coherence has been also employed to characterize the forest cover in the Colombian Amazon [R67]. In conjunction with polarimetric techniques, i.e., Polarimetric SAR Interferometry (PolInSAR), the interferometric coherence is employed to retrieve the forest vegetation [R53] or the crop plants [R68] heights.

All the techniques listed in the previous paragraph rely on a correct estimation of the coherence parameter. The estimated coherence values are overestimated, especially for low coherence values [R69]. Under the homogeneity hypothesis, the coherence accuracy and bias depend on the extend of the averaging or estimation process, in such a way that the larger the number of averaged pixels, the higher the coherence accuracy and the lower the bias. Therefore, since coherence accuracy is achieved at the expense of spatial resolution and spatial details, this point represents a clear trade-off for coherence estimation. Coherence estimation techniques rely also on the hypothesis that all the signals involved into the estimation process are stationary and in particular locally stationary processes. When this is not the case, biased coherence values result [R69]. Hence, a lack of signal stationarity can be considered as a second source of bias for coherence estimation. The departure of the stationarity condition may be induced by systematic phase variations mainly due to the terrain topography, but also to atmospheric effects or to deformation gradients. The most reliable technique to eliminate this bias is to compensate for the topography by means of external DEMs. Nevertheless, the DEM may not be available for the scene under study, or its quality may be rather low for

coherence estimation purposes. There exist alternative coherence estimation techniques aiming to solve these problems with different level of success.

In order to obtain coherence it is necessary to estimate the values of the different expectation values involved in (1.53), by means of the ensemble average. Nevertheless, since there are not multiple realizations of the SAR images S_k and S_l, it is required S_k, S_l and $S_k S_l^*$ to be ergodic in mean [R69] to substitute the ensemble averages in the realizations space by the space averages in the image space. Hence, it is possible to estimate coherence by means of

$$\rho_{MLT} = \frac{\sum_{m=1}^{M}\sum_{n=1}^{N} S_k(m,n)\, S_l^*(m,n)}{\sqrt{\sum_{m=1}^{M}\sum_{n=1}^{N}\left|S_k(m,n)\right|^2}\sqrt{\sum_{m=1}^{M}\sum_{n=1}^{N}\left|S_l(m,n)\right|^2}} \tag{1.54}$$

where m and n refer to the image dimensions and M and N are the number of averaged pixels in each dimension, respectively. ρ_{MLT} receives the name of multilook coherence estimator and it corresponds to the maximum likelihood estimator of [R70]. Under the assumption that the SAR images S_k and S_l may be described by circular complex Gaussian probability density functions (pdfs), the statistics of ρ_{MLT} have been completely characterized [R32][R69]. The main drawback of ρ_{MLT} is that it overestimates coherence, especially for low coherence values and for small values of MN, that is, small averaging windows. A second problem which may appear for large windows is that the processes S_k, S_l and $S_k S_l^*$ can be non-stationary within the analysis window, resulting in meaningless estimated coherence values.

2 Speckle Noise Filtering

2.1 Introduction

As it has been explained previously, a PolSAR system measures the scattering matrix $\mathbf{S}$ for every pixel. In the case of deterministic or point scatterers, this matrix determines completely the scattering process and it can be directly employed to retrieve physical information of the scatterer. Nevertheless, in case of distributed scatterers, the scattering matrix $\mathbf{S}$ is no longer deterministic but random due to the complexity of the scattering process. As indicated, this random behavior is referred to as speckle. Speckle is a true scattering measurement, but the complexity of the scattering process makes it necessary to consider it as a noise source. Consequently, the information of interest is no longer the scattering matrix, but the different stochastic moments necessary to specify completely the probability density function of the SAR data. These moments must be estimated from the measured data, or said in a different way, speckle noise must be filtered out or even eliminated to grant access to these statistical moments. In the case of PolSAR data, under the assumption of the vector $\mathbf{k}$ to be distributed according to the zero-mean, complex Gaussian distribution (1.28), these moments correspond to the covariance $\mathbf{C}$ or the coherency $\mathbf{T}$ matrices.

Section 1.4 already introduced the simplest approach to estimate the covariance or the coherency matrices, known as multilook (1.43), which corresponds to an incoherent average or a spatial average. Despite the multilook approach corresponds to the maximum likelihood estimator of the covariance or coherency matrices, it present the drawback that the estimation of the data is obtained at the expense of degrading the spatial resolution and the spatial details of the data. Figure 2.1 shows an example of these effects.

Considering the limitations of the multilook filtering approach, it is necessary to define different filtering alternatives that improve the multilook approach in such a way that they able to retain the spatial resolution and the spatial details of the image, but also leading to a correct and unbiased estimation of the covariance and coherency matrices.

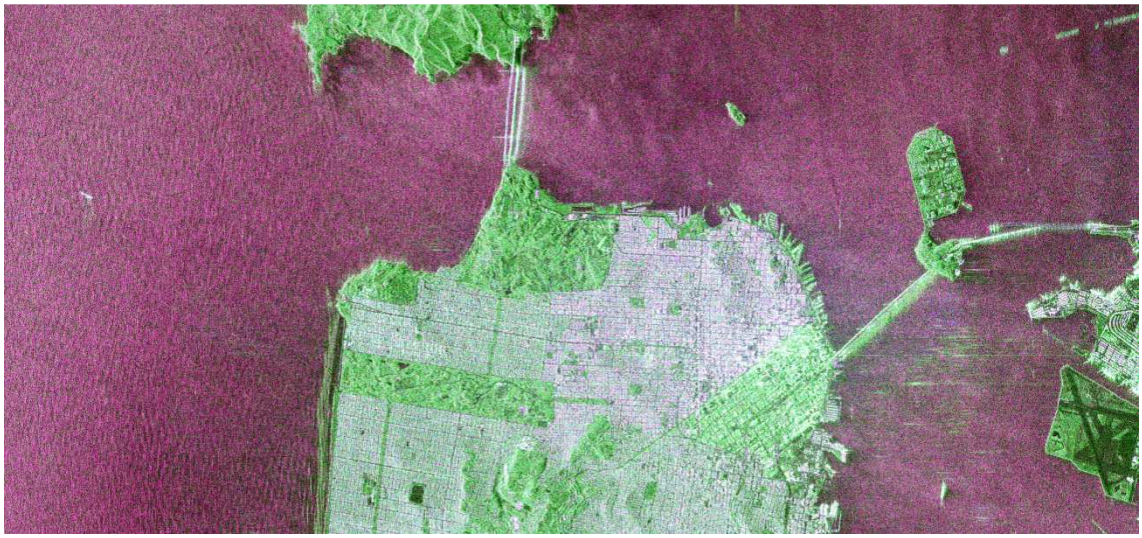

(a)

(b)

Figure 2.1 – Radarsat-2 polarimetric RGB image over San Francisco (USA) where the colour code is: S_{hh} blue, S_{vv} red and S_{hv} green. (a) Original image and (b) Filtered image with a 7×7 multilook filter.

2.2 PolSAR Speckle Noise Filtering Principles

The objective of any PolSAR speckle noise filter to be defined is to estimate the covariance or the coherency matrix while retaining the spatial resolution and the spatial details of the data. From a general point of view, it would be necessary to determine the general principles a PolSAR filter should follow in order to perform a correct estimation of the information of interest. Different authors have addressed the necessity to specify the general principles of a PolSAR speckle filter and which are the potential limitations: Touzi *et al.* [R73], Lee *et al.* [R74] and López-Martínez *et al.* [R75].

In the previous three references, as the data is assumed to be characterized by the zero-mean, complex Gaussian pdf, the information to retrieve is on the second order moments of the PolSAR data. In [R73], the authors propose the use of the Müeller matrix, despite they also consider the covariance matrix. In [R74] and [R75], the filtering is performed on

the covariance or on the coherency matrices. In any case, the use of the covariance, the coherency or the Müeller matrices to filter the data is equivalent as all these matrices contain the same information. For instance, as indicated previously, the covariance and the coherency matrices are related by similarity transformations. Implicitly, the authors are considering that these matrices contain all the necessary information to characterize the PolSAR data. This assumption is only valid under the hypothesis of (1.28), which only applies in case of stationary data. The presumption of more evolved stochastic data models, that may take into account additional signal variability, as for instance texture, are always associated with the necessity to estimate additional stochastic moments associated to the texture information.

Another point in which all the previous three references are in agreement is the need to consider the estimation of the previous matrices locally, adapting to the stationarity or homogeneity of the PolSAR data. This requirement is justified from two different points of view. The first one refers, due to the stationarity of PolSAR data, to the need to maintaining the spatial resolution and the radiometric information in case of point or deterministic scatterers, which may be extended to the idea of preserving the spatial resolution and the spatial details of the PolSAR data. The second refers to the fact that in case of distributed scatterers, the covariance matrix must be estimated on stationary data, avoiding the mixture of different stationary areas. This idea implies that the PolSAR filter must adapt the filtering process to the morphology of the PolSAR. The differences between the filtering principles for PolSAR data proposed by [R73], [R74] and [R75] are on how to consider the information that may be provided by the off-diagonal elements of the covariance or coherency matrices, and whether this information may be employed to optimize speckle noise reduction or not. The approaches proposed by [R73] and [R74] suggest an extension of the multiplicative speckle noise model, that applies for the diagonal entries of the covariance matrix, to the off-diagonal ones, despite it is also admitted that this extension may not lead to an optimum filtering of the speckle noise component. In [R74], the authors even propose that the use of the degree of statistical independence between elements must be avoided in order to avoid crosstalk, and that all the elements of the covariance matrix must be filtered by the same amount. These principles were extended in [R75], based on a more accurate PolSAR speckle noise model for the off-diagonal elements of the covariance matrix [R71][R72]. This model predicts that for a given off-diagonal element of the covariance matrix, speckle presents a complex additive nature for low coherence values, whereas speckle tends to be multiplicative in case of high coherences. Consequently, an optimum speckle noise reduction should adapt to the type of noise for the off-diagonal elements of the covariance matrix, that is, filtering must adapt to the level of coherence. As it may be concluded, a PolSAR filters needs also to be adapted to the polarimetric information content of the data. Consequently, in connection with what has been explained previously, the way a PolSAR filter adapts to the local information must consider all the information provided by the covariance or coherency matrices.

2.3 PolSAR Speckle Noise Filtering Alternatives

As indicated in Section 1.4, the first alternative to estimate the covariance or the coherency matrices is to consider their maximum likelihood estimator that corresponds to an incoherent spatial average as expressed in (1.44). In this case, the estimation of the information is obtained at the expense of the loss of spatial resolution and spatial details. Consequently, in order to avoid the previous drawbacks, the PolSAR data filters should adapt to the morphology of the SAR image to retain the spatial details, while leading to a correct and unbiased estimation of the covariance or coherency matrices.

PolSAR images are inherently heterogeneous as they reflect the heterogeneity of the Earth surface. Consequently, a first alternative to adapt to this heterogeneity, in order to avoid the loss of spatial resolution and spatial details, is to adapt locally to the signal morphology. One option to achieve this local adaptation is to consider edge aligned windows, as proposed in [R74]. Previously to the PolSAR data filtering process, the algorithm in [R74], known as *Refined Lee Filter*, proposed the use of a directional masks, within the analysis window, to determine the most homogeneous part of the sliding window where the local statistics have to be estimated. This spatial adaptation permits to preserve relatively sharp edges and local details. Once the directional mask defines the homogeneous pixels that have to be employed to estimate the covariance or the coherency matrix, these are estimated by means of the Local Linear Minimum Mean Mean Square Error (LLMMSE) approach, i.e.,

$$\hat{\mathbf{Z}} = \overline{\mathbf{Z}} + b\left(\mathbf{Z} - \overline{\mathbf{Z}}\right) \tag{2.1}$$

where $\hat{\mathbf{Z}}$ is the estimated value of the covariance matrix, $\overline{\mathbf{Z}}$ is the local mean covariance matrix computed with the homogeneous pixels selected by the edge aligned window and $\mathbf{Z}$ corresponds to the covariance matrix of the central pixels. Finally, b is a weighting function having a value between zero and one derived from the statistics of the Span image. Over homogeneous areas, $b \approx 0$ so the estimated covariance matrix corresponds to the values of the local means as it would be expected in absence of spatial details. Nevertheless, in the case the central pixel of the analysis window corresponds to a deterministic scatterer $b \approx 1$ producing $\hat{\mathbf{Z}}$ to be the covariance matrix of the scattered. Consequently, the pixel is not filtered and the spatial resolution is preserved, as observed in Figure 2.2. In relation with the filtering procedure proposed in [R74], the authors proposed also a filtering alternative where the pixels to be averaged within the analysis window are those with the same scattering mechanism as the central pixel, obtained through the Freeman-Durden decomposition [R77].

Figure 2.2 – Radarsat-2 polarimetric RGB image over San Francisco (USA) where the colour code is: S_{hh} blue, S_{vv} red and S_{hv} green. Filtered image with the LLMMSE speckle filter.

As it may be observed, the previous filtering approach adapts to the signal morphology through a family of edge aligned windows. Hence, the adaptation to the signal morphology is restricted to a finite family of aligned windows. In [R76], the authors extended the ideas presented in [R74], but instead to consider edge aligned windows, the authors

introduced the concept to *region growing* to define an adaptive set of homogeneous pixels surrounding the pixel under analysis in order to adapt to the local morphology of the data. As in the case of [R74], the adaptation to the signal morphology is achieved through the Span image. The region growing process is based on comparing a given pixel against its neighbors to determine their similarity by considering their corresponding covariance and coherency matrices. Since a PolSAR system provides for every pixel only the scattering matrix, an initial process of regularization that assures full-rank covariance or coherency matrices is necessary. This regularization process could be performed with the multillok filter, but it would introduce a loss of spatial resolution and spatial details. In [R74], the authors propose the use of the median filter. Nevertheless, this alternative introduces a bias in the estimated data, as in the case of non-symmetric distributions, such the one of the amplitude or the intensity of a SAR image or the one of the Span, the median does not correspond to the mean.

All the previous filtering approaches adapt to the signal morphology locally under the assumption that the pixels surrounding the pixel of analysis present a high probability to be statistically similar. Hence, these filters assume that the data are locally stationary. Nevertheless, it has been recently demonstrated that this idea of local stationary could be relaxed under the assumption that similar pixels to the one of analysis are available not only on the neighborhood of the pixel of analysis, but on the complete image [R78].

Figure 2.3 – Radarsat-2 polarimetric RGB image over San Francisco (USA) where the colour code is: S_{hh} blue, S_{vv} red and S_{hv} green. Filtered image with the BPT speckle filter.

In order to increase the filtering effect, one option, as shown in [R76], is to increase the number of homogeneous pixels to be averaged that are similar to the pixel under consideration. In [R76], as well as in [R74], the similarity is measured considering only the information contained in the diagonal elements of the covariance or coherency matrices. Therefore, these approaches neglect the information provided by the off-diagonal elements of these matrices. The way to take into account all the information provided by the covariance or the coherency matrices is to consider the concept of the *distance* in the space defined by the matrices themselves. This approach has been considered in [R78] as well as in [R79]. In [R79], the authors propose to introduce the concept of *Binary Partition Tree* as a hierarchical structure to exploit the relations that may be established between similar pixels. In essence, the filtering alternative proposed in [R79] produces first a binary partition tree that established the relations between similar pixels on the basis of a distance that takes into account all the polarimetric information. In a second step, the binary partition tree is pruned to find the largest homogeneous regions of the image. This filtering alternative allows to filter large homogeneous areas, while maintaining the spatial details if the data as observed in Figure 2.3.

The objective of all the previous filtering techniques is to obtain the best estimate of the covariance or coherency matrices by means of increasing the number of averaged samples. Nevertheless, if the number of available homogeneous pixels is not large enough, the way to improve the estimation of the covariance and coherency matrices must be address by considering a better exploitation of the Wishart distribution. As shown in [R71] and [R72], the Wishart distribution allows defining the multiplicative-additive speckle noise model for all the elements of the covariance or the coherency matrices. This model has been exploited for PolSAR data filtering in [R75], where it is demonstrated that if the filtering process is adapted to the multiplicative or additive nature of speckle, depending on the correlation of a pair of SAR images, it may lead to an improved estimation of the different parametric parameters that characterize the covariance or coherency matrices.

Beyond all the PolSAR data filtering techniques presented in this Section, there exist a wide variety of similar approaches in the related literature, where a comparison among some of them has been presented in [R80] and [R81]. Nevertheless, it may be concluded that reaching an optimal compromise of a joint preservation of the polarimetric and the spatial information, in case of PolSAR data filtering, is still today a problem without an adequate solution. Consequently, the selection of a particular filtering alternative for PolSAR data must take into consideration the final application of the PolSAR data in order to determine the optimum filtering according to that application.